Repetitive Periodic Motion Planning and Directional Drag Optimization of Underwater Articulated Robotic Arms

Bong-Huan Jun, Jihong Lee, and Pan-Mook Lee

Abstract: In order to utilize hydrodynamic drag force on articulated robots moving in an underwater environment, an optimum motion planning procedure is proposed. The drag force acting on cylindrical underwater arms is modeled and a directional drag measure is defined as a quantitative measure of reaction force in a specific direction in a workspace. A repetitive trajectory planning method is formulated from the general point-to-point trajectory planning method. In order to globally optimize the parameters of repetitive trajectories under inequality constraints, a 2-level optimization scheme is proposed, which adopts the genetic algorithm (GA) as the 1st level optimization and sequential quadratic programming (SQP) as the 2nd level optimization. To verify the validity of the proposed method, optimization examples of periodic motion planning with the simple two-link planner robot are also presented in this paper.

Keywords: Directional drag, drag optimization, repetitive motion planning, underwater robot.

1. INTRODUCTION

In recent years, underwater robot technologies have been evolved to satisfy the wide and various requirements for underwater missions. Despite such progress in underwater robot technologies, the missions are still in need of robots with more versatile capabilities and higher efficiency. In order to enhance the capabilities and efficiency of underwater robots, a great deal of attention has been attracted to the locomotion of underwater creatures such as fishes, marine mammals, and aquatic insects. Many pervious studies have been carried out to utilize the mechanism of underwater animals for underwater robots. Various swimming modes of fishes are enumerated and the analytical method for their propulsive mechanism is overviewed in [1]. In [2-6], the propulsive and maneuvering locomotion of fish is studied and imitated for enhancing the performance and efficiency of underwater vehicles. Previous work [3] attempted to determine the relation between the performance of the fish robot and the motion of the tail fin based on experimental study. The tail of the fish robot has two links at the tail peduncle and the tail fin. The frequency, amplitude, and phase of motion of joints are investigated for better propulsion and turning performance in the study. However, the mathematical model of the articulated link is not constructed and there is no consideration of the mathematical dynamic model of links in the works. Previous work [6] assessed the swimming speed and turning performance of rigid biological systems with a high-speed video system. It is observed in the study that the whirligig beetles, which propel themselves by drag-stroke of 2-link paddle-like legs shown in Fig. 1, can swim up to 0.55 m/s. But it has not been attempted to utilize the drag force with rigid robotic arms by mimicking the beetles.

The purpose of this study is to find the optimal drag-stroke of articulated robots to utilize the reaction drag force. The motion of the whirligig beetle introduced in [6] might be one of several good examples to explain the purpose of this problem. The concept of the purpose is depicted as in Fig. 2. As shown there, the problem to be solved in this study is to find a trajectory of articulated underwater arms maximizing total drag force in a specific direction during a period of motion.

The studies on underwater manipulators are found in [7-9] and the references are there-in. The modeling of underwater manipulators is carried out for efficient dynamic simulation in [7]. Because the authors are focused on the efficient calculation of dynamics, iterative N-E equations of motion are adopted in the study. Path planning of the underwater-vehicle-

Manuscript received February 28, 2005; revised September 7, 2005; accepted December 1, 2005. Recommended by Editor Jae-Bok Song under the direction of past Editor-in-Chief Myung Jin Chung. This work was supported by the Ministry of Marine Affairs and Fisheries (MOMAF) of Korea for the development of deep-sea unmanned underwater vehicle.

Bong-Huan Jun and Pan-Mook Lee are with the Maritime and Ocean Engineering Research Institute (MOERI), a branch of the Korea Ocean Research and Development Institute (KORDI), Daejeon 305-343, Korea (e-mails: {bhjeon, pmlee} @moeri.re.kr).

Jihong Lee is with the Mechatronics Engineering Department, Chungnam National University, Daejeon 305-764, Korea (e-mail: jihong@cnu.ac.kr).

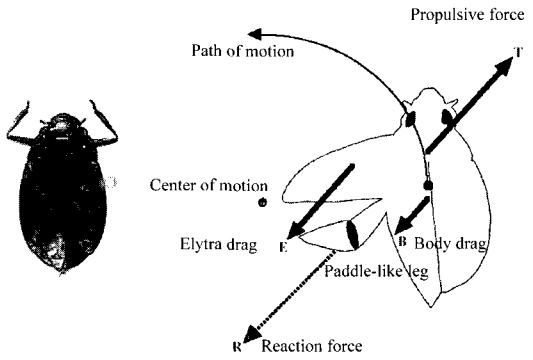

Fig. 1. Whirligig beetle (figure from [6]).

manipulator-system (UVMS) is treated in [8]. In the works, total drag encountered by the UVMS is minimized by the resolution of kinematic redundancy. Basically, since the method is based on the gradient of quadratic function of drag, the method solves the local optimization problem. On the other hand, a large number of approaches are reported to investigate the optimal trajectories of industrial manipulators on land to enhance their performance [10-13]. Most of them have treated the problem of point-to-point trajectory planning or the collision avoidance problem. Therefore, they have adopted the traveling time or power consumption of manipulators as an objective to be optimized. In [13], the deformation of the flexible manipulator is optimized for trajectory planning.

In this paper, an optimum motion planning procedure is proposed to utilize hydrodynamic drag force on articulated underwater robots. The drag force acting on cylindrical links is modeled as variables of joint angles, joint velocities, and fluid velocities explicitly, which may be convenient to manipulator analysis in off-line. As a quantitative measure of drag force in a specific direction in a workspace, a measure of directional drag of articulated underwater robots is proposed. Repetitive trajectory planning in joint space is formulated from the general point-to-point trajectory planning method by enforcing the end point of the trajectory to the start point with continuity condition.

To establish optimal trajectory of underwater arms, the parameters composing coefficients of the trajectory polynomial are searched by optimization procedure with adaptation of the directional drag measure as an objective function. In order to search the optimal solution efficiently, we propose a 2-level optimization procedure. Two level optimization uses the sequentially genetic algorithm (GA) and sequential quadratic programming (SQP) as optimization tools for constrained and bounded global optimization problems. To verify the validity of the proposed method, an example of optimal periodic motion planning of a simple two-link planner robot is presented.

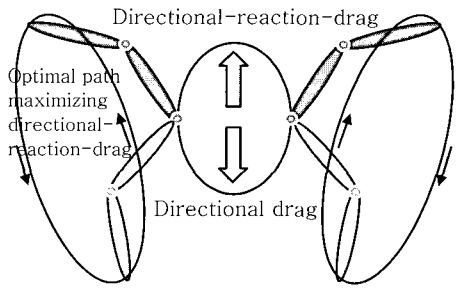

Fig. 2. Concept of drag utilization of articulated underwater robot by optimizing directional drag force.

In the following Section 1, generalized drag torque of underwater manipulators is described by joint angles and velocities, and then the directional drag force is defined. Repetitive trajectory planning is derived from general point-to-point trajectory planning in Section 2 while optimization using the 2-level procedure is described in Section 3. Section 4 is devoted to case studies of the proposed method and concluding remarks are made in Section 5.

2. DIRECTIONAL DRAG FORCE

In this section, the dynamics of articulated underwater robots are briefly reviewed and the hydrodynamic drag term in the dynamic equation is modeled by describing drag torque using the fluid velocities, joint angles, and joint velocities under several assumptions for simplicity. The drag torque is transformed to the drag force in a workspace using the Jacobian and inertial matrix of robots. Projecting the workspace drag force to an arbitrary direction vector, we define a measure of directional drag force in a workspace, which can be used as an index to evaluate magnitude of drag force in a specific direction with respect to workspace coordinates. This measure is used in Section 4 as an objective function for drag optimization.

2.1. Dynamics of underwater robots

When the n degrees-of-freedom articulated robot moves in an underwater environment, the dynamic equation of the robot can be described as

$$\mathbf{M}(\mathbf{q})\ddot{\mathbf{q}} + \mathbf{C}(\mathbf{q}, \dot{\mathbf{q}}) + \mathbf{D}(\mathbf{q}, \dot{\mathbf{q}}) + \mathbf{G}(\mathbf{q}) = \boldsymbol{\tau}, \quad (1)$$

where $\mathbf{M} \in \Re^{n \times n}$ is inertia matrix including added mass, $\mathbf{C} \in \Re^n$ is the Coriolis and centrifugal term caused by rigid body and added mass, $\mathbf{D} \in \Re^n$ is hydrodynamic drag and lift force term, $\mathbf{G} \in \Re^n$ is the buoyancy and gravity term, and $\boldsymbol{\tau} \in \Re^n$ is the joint torque vector.

The hydrodynamic drag force acting on a rigid

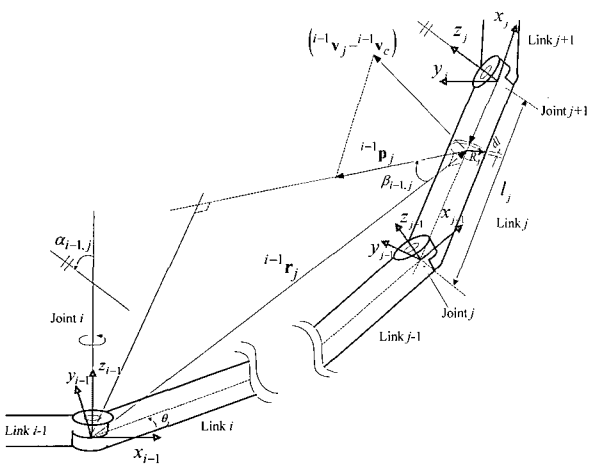

Fig. 3. Link coordinate system of underwater arm.

body can be decomposed into shear drag and pressure drag. Since the shear drag will be small for an underwater robot, we handle only the pressure drag as many previous works have done [7,9,17]. For simplicity, we assumed that the lift force resulting from the robot posture is negligible, that all of the links are cylindrical solid, and that the cylinders are fully submerged in addition to the lumped approximation for the forces and the assumption of unbounded and irrotational fluid. Then, the drag term **D** in (1) is to be a function of joint angles, joint velocities, fluid velocity, and hydrodynamic coefficients determined by the geometries of the links. To describe the drag term explicitly, the approach starts from the link coordinate system shown in Fig. 3.

Assuming the j-th link is partitioned into disk slices with small thickness of dl, we can write the drag force acting on a disk in fluid with respect to the (i-1)-th coordinate system as

$$d\,{}^{i-1}d_j = -\rho C_{Dj} R_j \,|\,{}^{i-1}p_j\,|\,{}^{i-1}p_j dl\,, \tag{2}$$

where ρ is water density, C_{Dj} and R_j are drag coefficient and radius of j-th link respectively, and ${}^{i-1}p_j$ is magnitude of translational velocity vector normal to the edge of disk expressed in (i-1)-th coordinates. ${}^{i-1}\mathbf{p}_j$, which can be obtained by projecting the relative disk velocity with respect to velocity of fluid to the unit vector in the y-axis of j-th coordinates as

$${}^{i-1}p_j = ({}^{i-1}\mathbf{v}_j - {}^{i-1}\mathbf{v}_c)^{\mathrm{T}}\ {}^{i-1}\mathbf{e}_{jy}\,, \tag{3}$$

where ${}^{i-1}\mathbf{v}_j$ and ${}^{i-1}\mathbf{v}_c$ are velocity vectors of disk and fluid with respect to the (i-1)-th frame, respectively. $(\cdot)^T$ is vector transpose, and ${}^{i-1}\mathbf{e}_{yj}$ is y-axis unit vector of j-th link coordinates expressed in (i-1)-th coordinates. As the surface integral can be replaced with line integral by strip theory, drag force on the j-th link expressed in the (i-1)-th coordinate system can be written as

$${}^{i-1}d_j = -\rho C_{Dj} R_j \int_0^{l_j} |\,{}^{i-1}p_j\,|\,{}^{i-1}p_j dl\,. \tag{4}$$

Then, the drag torque on the i-th joint caused by drag force on the j-th link can be written as

$$\tau_{di,j} = -\rho C_{Dj} R_j \cos\alpha_{i-1,j} \int_0^{l_j} {}^{i-1}r_j \cdot \sin\beta_{i-1,j}\,|\,{}^{i-1}p_j\,|\,{}^{i-1}p_j dl\,, \tag{5}$$

where $\alpha_{i-1,j}$ is twist angle between the z_{i-1} and z_j axis, ${}^{i-1}r_j$ is magnitude of ${}^{i-1}\mathbf{r}_j$, position vector from (i-1)-th frame to disk slice on j-th link, and $\beta_{i-1,j}$ is angle between ${}^{i-1}\mathbf{r}_j$ and ${}^{i-1}\mathbf{p}_j$.

Now, we get drag torque expressed by joint angles and velocities by introducing the relation between ${}^{i-1}\mathbf{v}_j$ and $\dot{\boldsymbol{\theta}}$ as

$${}^{i-1}\mathbf{v}_j = \sum_{k=1}^{j} {}^{i-1}\mathbf{U}_{jk}\dot{\theta}_k\,{}^{j}\mathbf{r}_j\,, \tag{6}$$

where

$${}^{i-1}\mathbf{U}_{jk} \equiv \frac{\partial}{\partial\theta_k}\,{}^{i-1}\mathbf{A}_j = \begin{cases} {}^{i-1}\mathbf{A}_{k-1}\mathbf{Q}^{k-1}\mathbf{A}_j & \text{for } k \le j \\ 0 & \text{for } k > j \end{cases}, \tag{7}$$

$$\mathbf{Q} = \begin{bmatrix} 0 & -1 & 0 & 0 \\ 1 & 0 & 0 & 0 \\ 0 & 0 & 0 & 0 \\ 0 & 0 & 0 & 0 \end{bmatrix}, \tag{8}$$

${}^{i-1}\mathbf{A}_j$ is homogeneous coordinate transformation matrix from (i-1)-th frame to j-th frame and ${}^{j}\mathbf{r}_j$ is position vector of disk slice on j-th link expressed in j-th frame. After replacing the definite integral in (5) with numerical integration, we substitute (6) into (3) and (3) into (5). Collecting all the drag forces affecting the i-th joint, we finally write the drag term in (1) as

$$\mathbf{D}(\boldsymbol{\theta},\dot{\boldsymbol{\theta}}) = [\tau_{d1},\cdots,\tau_{dn}]^T\,, \tag{9}$$

$$\begin{aligned} \tau_{di} &= \sum_{j=i}^{n} \tau_{di,j} \\ &= \rho \sum_{j=i}^{n} \left[C_{Dj} R_j \cos\alpha_{i-1} \cdot \sum_{x=1}^{s} \left({}^{i-1}r_{j,x} \sin\beta_{i-1,j} \left|{}^{i-1}p_j\right| {}^{i-1}p_j \frac{l_j}{s} \right) \right], \end{aligned} \tag{10}$$

$$ {}^{i-1}p_j = \left(\sum_{k=1}^{j} \left({}^{i-1}\mathbf{U}_{jk}\dot{\theta}_k \, {}^{j}\mathbf{r}_{j,x} \right) - {}^{i-1}\mathbf{v}_c \right)^T {}^{i-1}\mathbf{A}_j \mathbf{e}_y . \quad (11) $$

where s is number of disk slices and ${}^{i-1}r_{j,x}$ is magnitude of position vector, ${}^{i-1}\mathbf{r}_{j,x}$, from (i-1)-th coordinate system to x-th slice of j-th link.

2.2. Directional drag force in task space

The drag term derived in the previous section is transformed to the drag force in a workspace using the Jacobian and inertial matrix of robots. Projecting the drag force to the directional vector, we define a measure of directional drag force in this subsection.

Assuming that an n-degrees-of-freedom robot is working in an m-dimensional workspace, we can generally express the relationship between joint velocity vector, $\dot{\boldsymbol{\theta}} \in \Re^n$, and end-effector velocity, $\dot{\mathbf{r}}$, using Jacobian matrix $\mathbf{J}(\theta)$ by

$$ \dot{\mathbf{r}} = \mathbf{J}(\boldsymbol{\theta})\dot{\boldsymbol{\theta}} . \quad (12) $$

Differentiating (12) with respect to time and using (1) we get the following dynamic equation in a workspace.

$$ \ddot{\mathbf{r}} - \dot{\mathbf{J}}\dot{\boldsymbol{\theta}} + \mathbf{J}\mathbf{M}^{-1}(\mathbf{C}+\mathbf{G}) + \mathbf{J}\mathbf{M}^{-1}\mathbf{D} = \mathbf{J}\mathbf{M}^{-1}\boldsymbol{\tau} \quad (13) $$

The term $\mathbf{J}\mathbf{M}^{-1}\mathbf{D} \in \Re^m$ represents transformation of joint drag torque in a joint space to the end-effector acceleration in a workspace. Since this term is induced by drag forces of links, we refer to this term as '*drag acceleration*'. The drag acceleration in a specific direction of a workspace can be obtained by projecting the term to the direction vector by

$$ f_d = \mathbf{e}_d^T \cdot \mathbf{J}\mathbf{M}^{-1}\mathbf{D}, \quad (14) $$

where $\mathbf{e}_d$ is specific direction vector satisfying $\|\mathbf{e}_d\| = 1$. We define (14) as the '*directional drag acceleration*' of the end-effector. When the end-effector is accelerated by the directional drag acceleration, the reaction force acts on the base of the arm in the opposite direction, $-\mathbf{e}_d$. Neglecting the variation of mass matrix and assuming that the reaction drag force is proportional to the drag acceleration of the end-effector, we adopt the directional drag acceleration as a measure of the directional drag force.

In addition, as a measure of drag force efficiency, we define the drag force efficiency in a workspace. Since the right hand of (13) represents the total input acceleration caused by the total joint torque, we can define a measure of drag-force-efficiency by dividing (14) by total input acceleration in the workspace as

$$ E_{fd} = \frac{|\mathbf{e}_d^T \cdot \mathbf{J}\mathbf{M}^{-1}\mathbf{D}|}{\|\mathbf{J}\mathbf{M}^{-1}\boldsymbol{\tau}\|} . \quad (15) $$

3. REPETITIVE MOTION PLANNING

3.1. Quintic polynomial

In general trajectory planning problems of manipulators, the time history of all joint variables and their two time derivatives are planned to achieve desired motion. If initial and final conditions on joint angles, velocities, and accelerations are given, the quintic polynomial can be used for the planning of each joint trajectory. The quintic polynomial path of the j-th joint is described as

$$ \theta_j(t) = a_{j,0} + a_{j,1}t + a_{j,2}t^2 + a_{j,3}t^3 + a_{j,4}t^4 + a_{j,5}t^5 , \quad j = 1,\ 2,\ \cdots\ n, \quad (16) $$

where n is the number of joints and the unknown coefficient a_j can be determined from the known initial and final conditions. When a robot moves repetitively along the given periodic trajectory, the initial and final point share the same positions, velocities, and accelerations because of its continuity conditions. Replacing the final conditions ($\theta_{j,f}$, $\dot{\theta}_{j,f}$ and $\ddot{\theta}_{j,f}$) with the initial conditions ($\theta_{j,0}$, $\dot{\theta}_{j,0}$ and $\ddot{\theta}_{j,0}$), we have each of the coefficients in (16) as

$$ a_{j,0} = \theta_{j,0}, \quad (17) $$

$$ a_{j,1} = \dot{\theta}_{j,0}, \quad (18) $$

$$ a_{j,2} = \frac{\ddot{\theta}_{j,0}}{2}, \quad (19) $$

$$ a_{j,3} = \frac{-20\dot{\theta}_{j,0} - 2\ddot{\theta}_{j,0}T}{2T^2}, \quad (20) $$

$$ a_{j,4} = \frac{30\dot{\theta}_{j,0} + \ddot{\theta}_{j,0}T}{2T^3}, \quad (21) $$

$$ a_{j,5} = \frac{-6\dot{\theta}_{j,0}}{T^4}, \quad (22) $$

where T is time period of motion, and $\theta_{j,0}$, $\dot{\theta}_{j,0}$, and $\ddot{\theta}_{j,0}$ are initial angle, velocity and acceleration of j-th joint, respectively. Therefore, the trajectory optimization problem in the quintic polynomial is to find optimal initial conditions, $\theta_{j,0}$, $\dot{\theta}_{j,0}$, $\ddot{\theta}_{j,0}$ and time period T under the given joint and torque constraints.

3.2. 4-3-4 polynomial

If the positions of two via points are given, either the 4-3-4 or 3-5-3 polynomial can be used for motion planning. In the case of 4-3-4 polynomial trajectories, the j-th trajectory section of the i-th joint is described by

$$\theta_{i,j}(t) = A_{i,j,0} + A_{i,j,1}t + A_{i,j,2}t^2 + A_{i,j,3}t^3 + A_{i,j,4}t^4$$
$$i = 1, \cdots, n, \quad j = 1,\ 2,\ 3, \quad A_{i,2,4} = 0. \tag{23}$$

The t in (23) is normalized time variable defined with real time τ as

$$t = \frac{\tau - \tau_{j-1}}{\tau_j - \tau_{j-1}}, \tag{24}$$

where τ_j is real time at the start point of the j-th trajectory segment. The coefficients of 4-3-4 trajectories can be determined from the known position and continuity conditions with normalized time t as

$$A_{i,1,0} = \theta_{i,1}(0),\ A_{i,2,0} = \theta_{i,1}(1),\ A_{i,3,0} = \theta_{i,3}(0), \tag{25}$$
$$A_{i,1,1} = v_{i,1}(0)t_1,\ A_{i,2,1} = x_{i,3},\ A_{i,3,1} = x_{i,6}, \tag{26}$$
$$A_{i,1,2} = \frac{a_{i,1}(0)}{2}t_2,\ A_{i,2,2} = x_{i,4},\ A_{i,3,2} = x_{i,7}, \tag{27}$$
$$A_{i,1,3} = x_{i,1},\ A_{i,2,3} = x_{i,5},\ A_{i,3,3} = x_{i,8}, \tag{28}$$
$$A_{i,1,4} = x_{i,2}\ \ A_{i,2,4} = 0,\ A_{i,3,4} = x_{i,9}, \tag{29}$$

where $t_j = \tau_j - \tau_{j-1}$, and $x_{i,k}$ is the k-th element of the solution vector of the following linear algebraic equation.

$$\mathbf{C}_i\mathbf{x}_i = \mathbf{b}_i, \tag{30}$$

where $\mathbf{C}_i$ is banded structure matrix given as

$$\begin{bmatrix}
1 & 1 & 0 & & & & & & & \\
3 & 4 & -\frac{t_1}{t_2} & & & & & 0 & & \\
6 & 12 & 0 & -\frac{2t_1^2}{t_2^2} & & & & & & \\
 & & 1 & 1 & 1 & & & & & \\
 & & 1 & 2 & 3 & -\frac{t_2}{t_3} & & & & \\
 & & & 2 & 6 & 0 & -\frac{2t_2^2}{t_3^2} & & & \\
 & & & & & 1 & 1 & 1 & 1 & \\
 & & 0 & & & 1 & 2 & 3 & 4 & \\
 & & & & & & 2 & 6 & 12 &
\end{bmatrix} \tag{31}$$

and $\mathbf{b}_i$ is given as follows:

$$\mathbf{b}_i = [\delta_{i,1} - v_{i,1}(0)t_1 - \frac{a_{i,1}(0)}{2}t_1^2,\ \ -v_{i,1}(0)t_1 - a_{i,1}(0)t_1^2 \tag{32}$$
$$-\delta_{i,2},\ 0,\ 0,\ \delta_{i,3},\ v_{i,1}(0)t_3,\ a_{i,1}(0)t_3^2]^T,$$

where $\delta_{i,j} = \theta_{i,j}(1) - \theta_{i,j}(0)$. Note that the final velocity and acceleration are replaced with the initial ones in the last two elements of b_i because of the repetitive condition. Then the trajectory optimization problem becomes to find the initial condition, $\theta_{j,0}$, $\dot{\theta}_{j,0}$, $\ddot{\theta}_{j,0}$, via points, and time period of motion.

Even when there are more than two inter knot points, repetitive trajectories are easily planned based on general 3-3-3-3-3 or 3-···-3-5 polynomial trajectory planning methods. However, the larger number of optimizing parameters requires the longer time consumption of optimization process.

4. GLOBAL OPTIMIZATION STRATEGY

In this section, we discuss the optimization of repetitive motion taking into account dynamic equations of motion as well as bounds on joint positions, velocities, jerks and torques. Main difficulties of trajectory optimization of robotic arms come from the highly nonlinear-coupled dynamics and the high search dimension of trajectory space. The sequential quadratic programming, a representative nonlinear programming, is successfully used for constrained optimization with a bounded search space. However, the convergence of SQP depends highly on the initial estimation of solution because it uses the gradient information. Thus, it frequently may go into local minima for the highly nonlinear function unless there are many trials with various initial solutions.

The genetic algorithms of which detailed descriptions are found in [11,12,14,15] are adaptive, heuristic, probabilistic, iterative and global searching algorithms that mimic the mechanism of natural biological evolution. The GAs operate effectively on global optimization in a near optimal way because they find a population of solutions rather than a single solution. Moreover, GAs do not require a complete system model, and they can also perform multi-point searches. But unfortunately, their application is limited to the unconstrained optimization problem because there has been no method built into genetic algorithms for handling nonlinear equality or inequality constraints until now. One of the approaches to overcome the difficulty is to apply the penalty function, which gives a penalty to those solutions that violate constraints. However, the difficulties in determining the strength of the penalty leading to proper results still remains to be a problem.

In this study, we propose a global optimization scheme using both the GA and SQP. The GA searches overall solution space maximizing the fitness function with initial host population chosen randomly. The constraint is considered by the penalty function. We refer to this as 1st level optimization. Then the near optimal solution obtained from GA becomes the initial solution of SQP algorithm. The SQP completes the global optimization procedure by searching a fine optimal solution. We refer to this as 2nd level optimization from here on. In 1st level optimization, the inequality constraints are taken into account in the fitness function, ϕ, of GA as

$$\phi = f - \xi\sum_{i}^{k}\chi(|x_i| - 1), \tag{33}$$

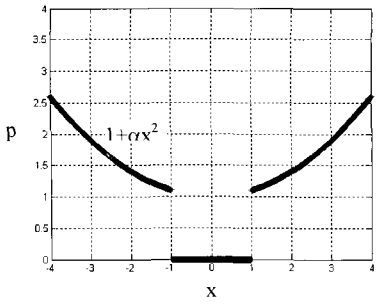

Fig. 4. Cost function for inequality constraints

where f is an objective function to be maximized in the GA, $(|x_i|-1)$ is normalized inequality constraints, k is number of inequality constraints, $\chi(\cdot)$ is a nonlinear function defined as

$$\chi(\cdot) \equiv \begin{cases} 0 & \text{when } |x_i| < 1 \\ 1+\alpha_i x_i^2 & \text{when } |x_i| > 1, \end{cases} \tag{34}$$

ξ is weight factor for the constraint that determines the strength of total penalty, while α_i is an individual weight factor that determines the contribution level of each constraint to the penalty function. The second term of right hand in (33) becomes penalty function p as depicted in Fig. 4.

In the repetitive trajectory planning problem of underwater robotic arms, total drag during periodic motion is the main concerning factor involved in the optimization. Since both joint angle and angular velocity affect the total drag, the optimization problem is then to find a combination of time series for joint angles and angular velocities in a time interval. If the situation in Fig. 2 is considered, the integration of directional drag can be an objective function as

$$f = \int_0^T \mathbf{e}_d^T \cdot \mathbf{J}\mathbf{M}^{-1}\mathbf{D}dt. \tag{35}$$

Adopting (35) as an objective function of the optimization process and $\mathbf{e}_d^T$ as the y-axis unit vector, we can find optimal periodic motion that maximizes drag in forward (downward) swing and minimizes drag in backward (upward) swing during a time period. If it is necessary to optimize the efficiency cost of the robotic arm, alternative objective function can be used using (15).

$$g = \int_0^T \frac{|\mathbf{e}_d^T \cdot \mathbf{J}\mathbf{M}^{-1}\mathbf{D}|}{|\mathbf{J}\mathbf{M}^{-1}\boldsymbol{\tau}|} dt \tag{36}$$

If the joint constraints are considered in the optimization process such as limitation of joint angles, angular velocities, accelerations, and torques, the optimization problem is described as follows:

Find optimal parameters, which minimizes the objective function given in (35) or (36) subject to:

$$\begin{aligned}
&\theta_{i,\min} \le \theta_i \le \theta_{i,\max} \quad (i=1,\cdots,n), \\
&\dot{\theta}_{i,\min} \le \dot{\theta}_i \le \dot{\theta}_{i,\max} \quad (i=1,\cdots,n), \\
&\ddot{\theta}_{i,\min} \le \ddot{\theta}_i \le \ddot{\theta}_{i,\max} \quad (i=1,\cdots,n), \\
&\dddot{\theta}_{i,\min} \le \dddot{\theta}_i \le \dddot{\theta}_{i,\max} \quad (i=1,\cdots,n), \\
&\tau_{i,\min} \le \tau_i \le \tau_{i,\max} \quad (i=1,\cdots,n).
\end{aligned} \tag{37}$$

Even though the bounds of joints in (37) are different from each other, they can be easily normalized so that they can be substituted to (34) by the following vector transformation.

$$\mathbf{x} \equiv \mathbf{D}\boldsymbol{\theta} + \mathbf{x}_0, \tag{38}$$

where $\theta=[\theta_1,\cdots,\theta_n]^T$, and

$$\mathbf{D} \equiv diag\left[\frac{2}{\theta_{1,\max}-\theta_{1,\min}} \cdots \frac{2}{\theta_{n,\max}-\theta_{n,\min}}\right], \tag{39}$$

$$\mathbf{x}_0 \equiv \left[-\frac{\theta_{1,\max}+\theta_{1,\min}}{\theta_{1,\max}-\theta_{1,\min}} \cdots -\frac{\theta_{n,\max}+\theta_{n,\min}}{\theta_{n,\max}-\theta_{n,\min}}\right]^T. \tag{40}$$

In quintic polynomial trajectory planning, the total parameters to be determined by the optimization process are the joint angles, angular velocities, angular accelerations of initial point, and period time of motion ($3n+1$ parameters). In 4-3-4 trajectory planning, joint angles, angular velocities, angular accelerations of initial point, and joint angles of two intermediate points ($5n$ parameters) need to be determined when the time period and execution time of each trajectory segment is fixed. If total execution time is fixed but time of each segment is not fixed, the total parameter becomes $7n$.

5. TWO-LINK ROBOT EXAMPLE

5.1. Drag Force on 2-link Robot

By using the proposed method, a repetitive polynomial trajectory of general n-dimensional articulated robotic arms can be planned subjected to the drag optimization.

In this section, a repetitive motion planning example using the quintic polynomial is described

Table 1. Parameters of planner 2-link robot.

Length of each link (l_i)	1 m
Radius of each link (R_i)	0.1 m
Water density (ρ)	1,000 kg/m^3
Mass of each link (m_i)	93.3 kg
Added mass of each link (m_{ia})	-9.3 kg
Drag coefficient of each link (C_{Di})	0.2

Table 2. Joint constraints of 2-link robot.

Item	Angle(degree)		Velocity(rad/s)		Accel.(rad/s^2)		Jerk(rad/s^3)		Torque(Nm)	
Joint	1	2	1	2	1	2	1	2	1	2
Max.	+1.57	+3.14	+1.05	+1.05	+1.57	+1.57	+2.5	+2.5	+250	+150
Min.	-1.57	-3.14	-1.05	-1.05	-1.57	-1.57	-2.5	-2.5	-250	-150

with a simple planner 2-link robot. Its link parameters are listed in Table 1 and joint constraints are shown in Table 2. We can calculate the inertia matrix, Coriolis and centrifugal term and drag term from robot parameters using the following equations.

$$\mathbf{M}=\begin{bmatrix} \frac{1}{3}\hat{m}_1 l_1^2+\frac{1}{3}\hat{m}_2+l_2^2+\hat{m}_2 l_1^2+\hat{m}_2 l_1 l_2\cos\theta_2 & \frac{1}{3}\hat{m}_2 l_2^2+\frac{1}{2}\hat{m}_2 l_1 l_2\cos\theta_2 \\ \frac{1}{3}\hat{m}_2 l_2^2+\frac{1}{2}\hat{m}_2 l_1 l_2\cos\theta_2 & \frac{1}{3}\hat{m}_2 l_2^2 \end{bmatrix} \quad (41)$$

$$\mathbf{C}=\begin{bmatrix} -\frac{1}{2}\hat{m}_2 l_1 l_2\dot{\theta}_1^2\sin\theta_2-\frac{1}{2}\hat{m}_2 l_1 l_2\dot{\theta}_1\dot{\theta}_2\sin\theta_2-\frac{1}{2}\hat{m}_2 l_1 l_2\dot{\theta}_2^2\sin\theta_2 \\ \frac{1}{2}\hat{m}_2 l_1 l_2\dot{\theta}_2^2\sin\theta_2 \end{bmatrix} \quad (42)$$

$$\mathbf{D}=\begin{bmatrix} \rho\left\{C_{D1}R_1\sum_{x=1}^{s}\left({}^0r_{1,x}\left|{}^0p_1\right|{}^0p_1\frac{l_1}{s}\right)+C_{D2}R_2\sum_{x=1}^{s}\left({}^0r_{2,x}\left|{}^0p_2\right|{}^0p_2\frac{l_2}{s}\right)\right\} \\ \rho C_{D2}R_2\sum_{x=1}^{s}\left({}^1r_{2,x}\left|{}^1p_2\right|{}^1p_2\frac{l_2}{s}\right) \end{bmatrix},$$

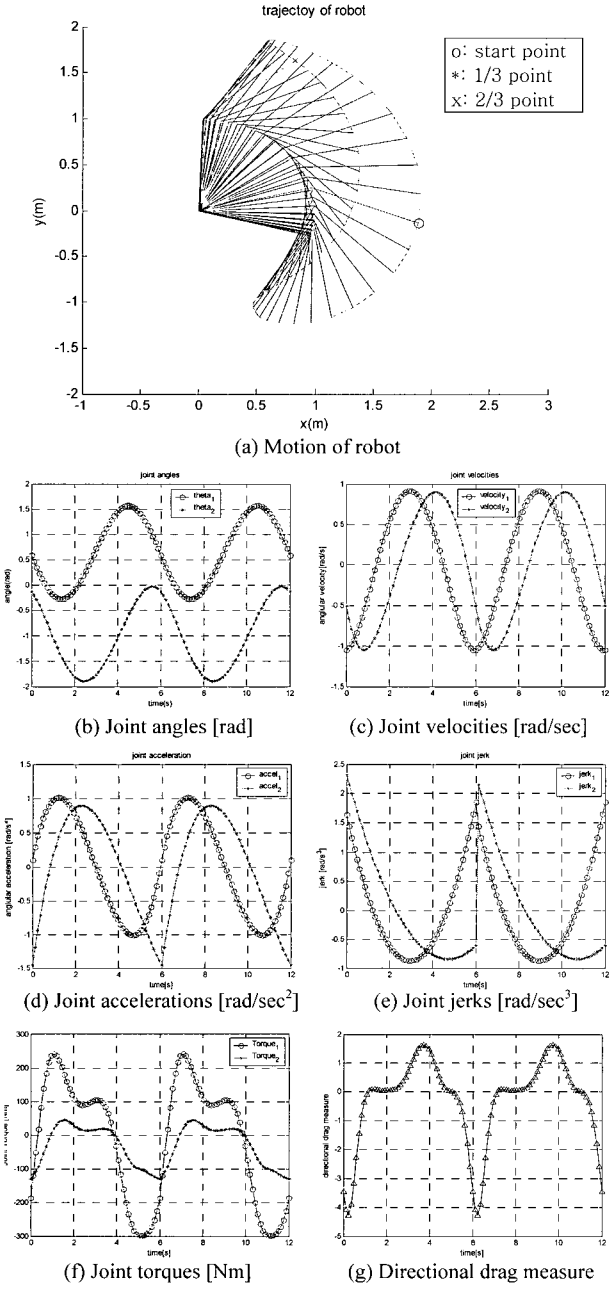

(a) Motion of robot
(b) Joint angles [rad]
(c) Joint velocities [rad/sec]
(d) Joint accelerations [rad/sec^2]
(e) Joint jerks [rad/sec^3]
(f) Joint torques [Nm]
(g) Directional drag measure

Fig. 5. Optimized trajectory by 1st level optimization (T=6s, $f=-1.5286$, g=0.1211).

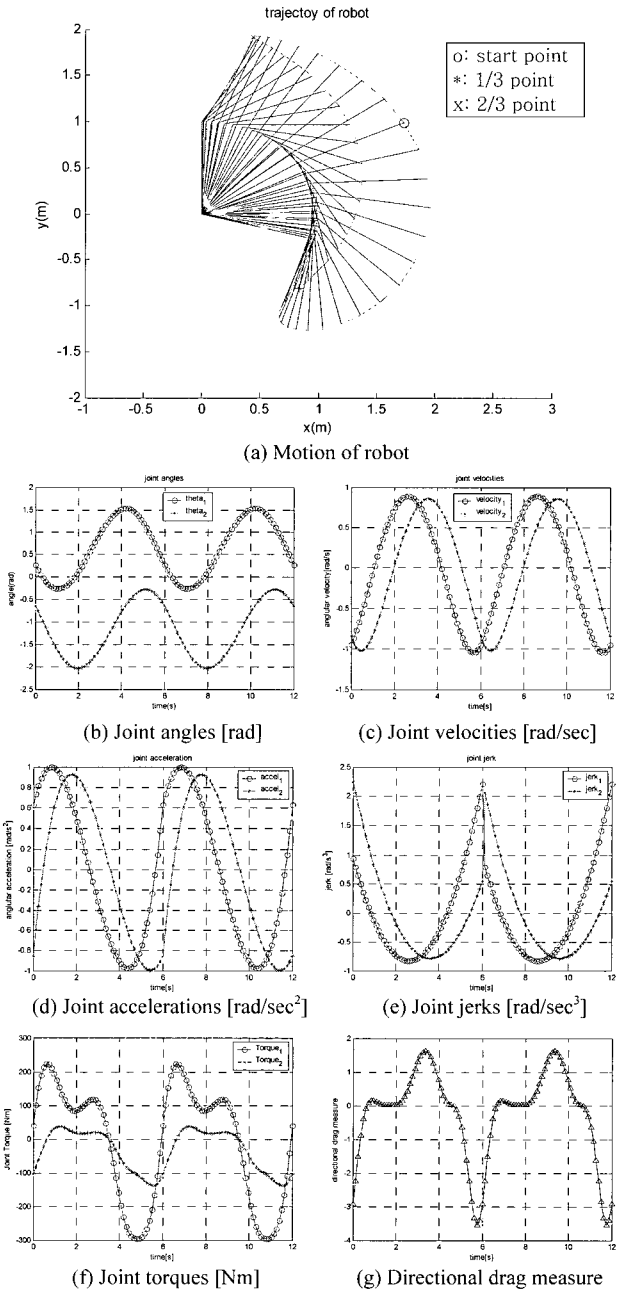

(a) Motion of robot
(b) Joint angles [rad]
(c) Joint velocities [rad/sec]
(d) Joint accelerations [rad/sec^2]
(e) Joint jerks [rad/sec^3]
(f) Joint torques [Nm]
(g) Directional drag measure

Fig. 6. Optimized trajectory by 2nd level optimization (T=6s, $f=-1.9558$, g=0.1613).

$$\begin{cases} {}^0p_1 = \left({}^0\mathbf{U}_{11}\dot{\theta}_1\,{}^0\mathbf{r}_{1,x} - {}^0\mathbf{r}_c\right)^T {}^0\mathbf{A}_1\mathbf{e}_y \\ {}^0p_2 = \left\{\left({}^0\mathbf{U}_{21}\dot{\theta}_1\,{}^0\mathbf{r}_{2,x}\right) + \left({}^0\mathbf{U}_{22}\dot{\theta}_2\,{}^0\mathbf{r}_{2,x}\right) - {}^0\mathbf{r}_c\right\}^T {}^0\mathbf{A}_2\mathbf{e}_y \\ {}^1p_2 = \left\{\left({}^1\mathbf{U}_{21}\dot{\theta}_1\,{}^1\mathbf{r}_{2,x}\right) + \left({}^1\mathbf{U}_{22}\dot{\theta}_2\,{}^1\mathbf{r}_{2,x}\right) - {}^1\mathbf{r}_c\right\}^T {}^1\mathbf{A}_2\mathbf{e}_y \end{cases} \tag{43}$$

where $\hat{m}_i = m_i - m_{ia}$, and the zero velocity of surrounding fluid is assumed.

If we neglect the buoyancy and gravity term, the dynamic equation of the underwater arm becomes

$$\boldsymbol{\tau} = \mathbf{M}\ddot{\boldsymbol{\theta}} + \mathbf{C} + \mathbf{D}. \tag{44}$$

5.2. First level trajectory optimization with GA

Fig. 5 shows the 1st level optimization results using GA with fitness function in (33). The directional vector that is the direction of drag to be optimized is chosen as unit vector in the y-axis of workspace coordinates. The weight factors ξ and α_i are chosen as 10 and 0, respectively. The time period of motion is fixed as 6 seconds. The GA is converged after about 50 generations. Optimized directional drag force f is -1.5286 and efficiency measure g is 0.1211. The time series of robot configurations resulted from optimization is depicted in Fig. 5(a). In Fig. 5(c), it is found that the lower extreme points of joint velocities

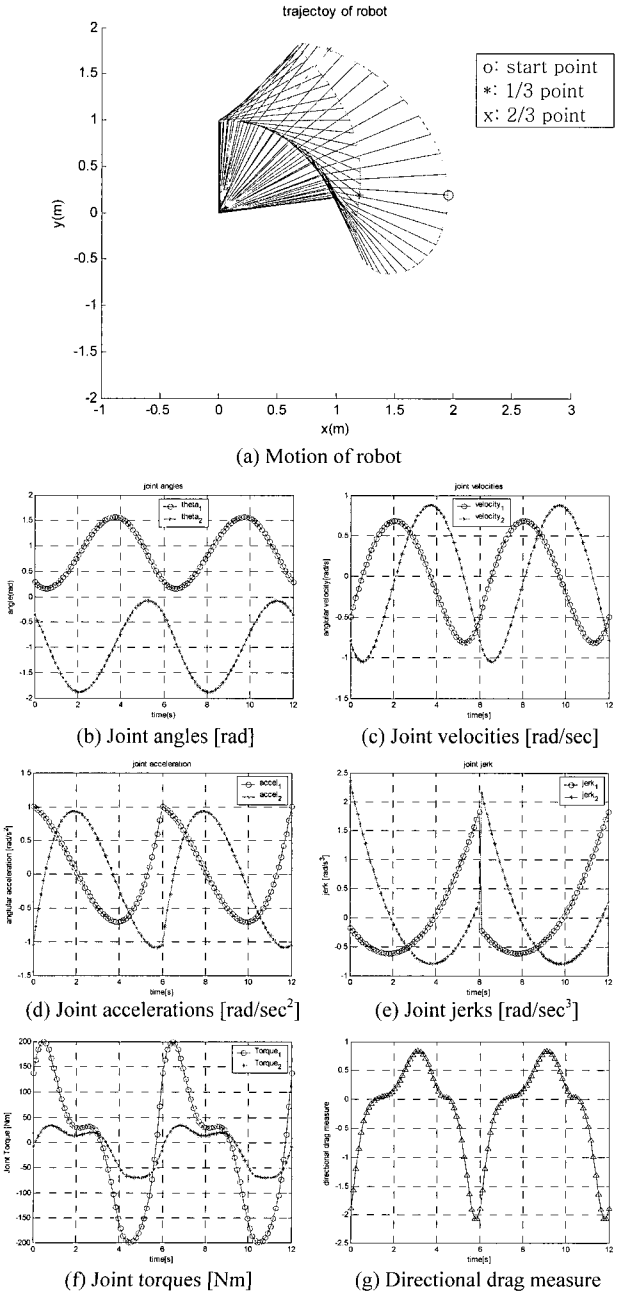

(a) Motion of robot

(b) Joint angles [rad]

(c) Joint velocities [rad/sec]

(d) Joint accelerations [rad/sec^2]

(e) Joint jerks [rad/sec^3]

(f) Joint torques [Nm]

(g) Directional drag measure

Fig. 7. Optimized trajectory with tight torque constraints (T=6s, $f = -1.2275$, g=0.1699).

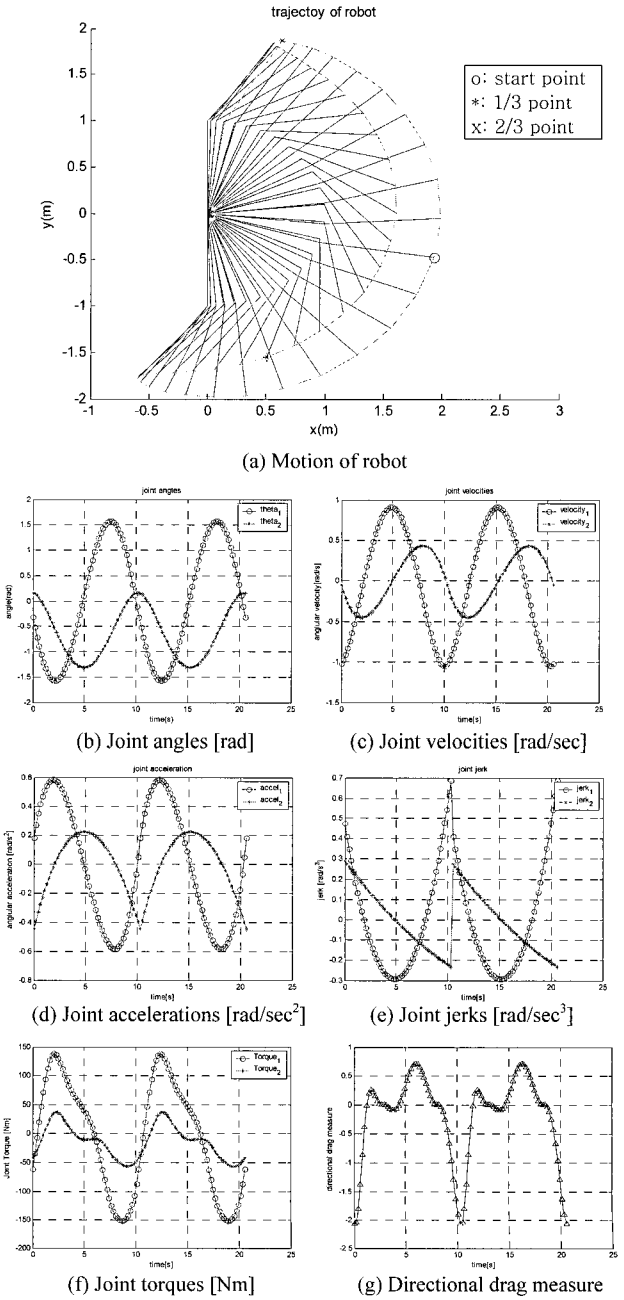

(a) Motion of robot

(b) Joint angles [rad]

(c) Joint velocities [rad/sec]

(d) Joint accelerations [rad/sec^2]

(e) Joint jerks [rad/sec^3]

(f) Joint torques [Nm]

(g) Directional drag measure

Fig. 8. Directional-drag & time-period optimized trajectory (T=10.29s, f=− 2.1159, g = 0.2363).

are reached at the lower bound of joint velocities. But Fig. 5 is near optimal solution rather than optimal solution. So we perform the 2nd level optimization procedure in the next subsection.

5.3. Second level trajectory optimization with SQP

Selecting the solution of 1st level optimization performed with GA as an input solution of SQP, we perform the 2nd level optimization procedure. The optimized results are shown in Fig. 6. The optimized directional drag f and efficiency measure g are -1.2275 and 0.1699, respectively. We verify that the objective function value is improved by about 30%

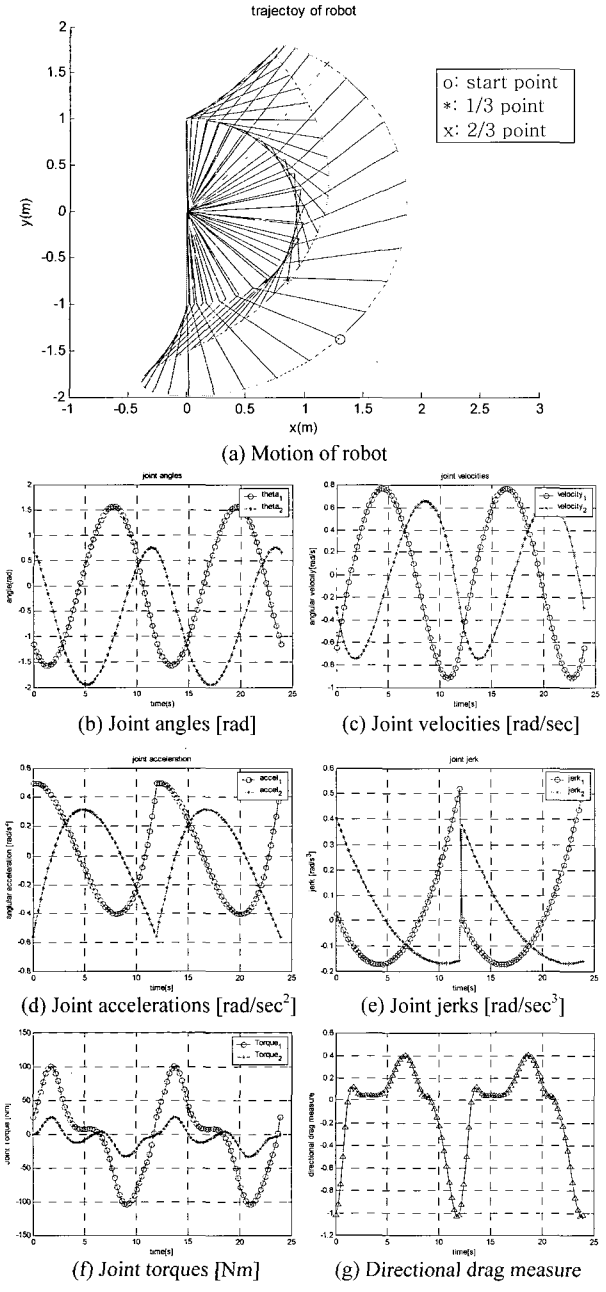

(a) Motion of robot

(b) Joint angles [rad]

(c) Joint velocities [rad/sec]

(d) Joint accelerations [rad/sec^2]

(e) Joint jerks [rad/sec^3]

(f) Joint torques [Nm]

(g) Directional drag measure

Fig. 9. Efficiency & time-period optimized trajectory (T=11. 96s, f =− 1.1900, g=0.2834).

via 2nd level optimization. Noting that the amplitude of velocities of Fig. 5 and Fig. 6 are nearly identical, we can find that the arm postures are more optimized in 2nd level optimization than in the 1st level. Fig. 7 shows the 2nd level optimization results when the joint torque is constrained more tightly as $|\tau_1| \le 200$ and $|\tau_2| \le 100$. As we can suppose, the swing angles of both joints and the velocity of the second joint are decreased due to the torque constraint of the first joint.

5.4. Optimal time period and optimal efficiency

In the previous subsections, the time period is fixed as 6 seconds in the optimization process. In this subsection the time period of swing motion is also optimized in the optimization process. Fig. 8 shows drag optimization results when the boundary of time period is given as $5 \le T \le 20$. Optimal directional drag force is obtained at 10.29 seconds of time period as -2.1159. The first joint angle swings fully from its lower limit to upper limit. The velocity constraint of the first joint is the main factor to restrict the drag force in this case.

When we choose the efficiency measure in (36) as an objective function, the optimization is resulted as indicated in Fig. 9. The optimized efficiency is 0.2834 while the directional drag is -1.1900 at 11.96 seconds of time period. Comparing Fig. 8(a) and (c) with Fig. 9(a) and (c), we verified that despite the affect of both postures and joint velocities to the drag force, the drag force is more dependant on the joint velocities, while the efficiency is more dependant on the joint postures.

6. CONCLUSION

As one way of utilizing hydrodynamic drag, the directional drag optimization method for periodic trajectories of underwater robotic arms is presented. Hydrodynamic drag force acting on underwater arms is modeled and a directional drag measure is defined as a quantitative measure in a specific direction of a workspace. The periodic motion planning method is formulated and the parameters of periodic trajectories are optimized adopting the proposed directional drag measure as an objective function. To find the global optimum solution of trajectories in the consideration of inequality constraints, a 2-level optimization procedure is presented. As 1st level optimization, the genetic algorithm searches globally near the optimal solution. The inequality constraints are taken into account by a penalty function proposed in this study. As 2nd level optimization, the sequential quadratic programming algorithm searches the fine optimal solution of the problem adopting the solution of 1st level optimization as an initial solution. From the simple 2-link example, it is verified that the periodic motion of an underwater arm is successfully planned and optimized with the proposed procedure.

Since the proposed method is developed under the assumption that the type of polynomial for trajectory is given, it is remained as a future work of the study to investigate whether the best polynomial or combination of polynomials gives the best trajectory.

REFERENCES

[1] M. Sfakiotakis, D. M. Lane, and J. B. C. Davies, "Review of fish swimming modes for aquatic locomotion," *IEEE J. of Oceanic Engineering*, vol. 24, no. 2, pp. 237-252, Apr. 1999.

[2] N. Kato, "Control performance in the horizontal plane of a fish robot with mechanical pectoral fins," *IEEE J. of Oceanic Engineering*, vol. 25, pp. 121-129, Jan. 2000.

[3] K. Hirata, T. Takimoto, and K. Tamura, "Study on turning performance of a fish robot," *Proc. of 1st International Symposium on Aqua Bio-Mechanisms*, pp. 287-292, Aug. 2000.

[4] J. M. Anderson, "The vorticity control unmanned underwater vehicle (VCUUV) performance results," *Proc. of 11th International Symposium on UUST*, vol. 11, pp. 360-369, Aug. 1999.

[5] I. Yamamoto, Y. Terada, T. Nagamatu, and Y. Imaizumi, "Propulsion system with flexible/rigid oscillating fin," *IEEE J. of Oceanic Engineering*, vol. 20, no. 1, pp. 23-30, Jan. 1995.

[6] F. E. Fish and A. J. Nicastro, "Aquatic turning performance by the whirligig beetle: Constraints on the maneuverability by a rigid biological system," *J. of Experimental Biology*, vol. 206, pp. 1649-1656, Aug. 2003.

[7] N. Sarkar and T. K. Podder, "Coordinated motion planning and control of autonomous underwater vehicle-manipulator systems subject to drag optimization," *IEEE J. of Oceanic Engineering*, vol. 26, no. 2, pp. 228-239, Apr. 2001.

[8] S. McMillan, D. E Orin, and C. S. G. Lee, "Efficient dynamic simulation of an underwater vehicle with a robotic manipulator," *IEEE Trans. on Systems, Man, and Cybernetics*, vol. 25, no. 8, pp. 1194-1206, Aug. 1995.

[9] G. Antonelli, S. Chiaverini, and N. Sarkar, "External force control for underwater vehicle-manipulator systems," *IEEE Trans. on Robotics and Automation*, vol. 17, no. 6, pp. 931-938, Dec. 2001.

[10] C.-S. Lin, P.-R. Chang, and J. Y. S. Luh, "Formulation and optimization of cubic polynomial joint trajectories for industrial robots," *IEEE Trans. on Automatic Control*, vol. 28, no. 12, pp. 1066-1074, Dec. 1983.

[11] W.-M. Yun and Y.-G. Xi, "Optimum motion planning in joint space for robots using genetic algorithms," *Robotics and Autonomous Systems*, vol. 18, no. 4, pp. 373-393, 1996.

[12] X. F. Zha, "Optimal pose trajectory planning for robot manipulators," *Mechanism and Machine Theory*, vol. 37, pp. 1063-1086, 2002.

[13] S. Yue, D. Henrich, W. L. Xu, and S. K. Tso, "Point-to-point trajectory planning of flexible redundant robot manipulators using genetic algorithms," *Robotica*, vol. 20, pp. 269-280, 2002.

[14] J. Holland, *Adaptation in Natural and Artificial Systems*, The University of Michigan Press, Ann Arbor, 1975.

[15] S. E. Carlson and R. Shonkwiler, "Annealing a genetic algorithm over constraints," *Proc. of International Conference on Systems, Man, and Cybernetics*, vol. 4. pp. 3931-3936, 1998.

[16] S. K. Agrawal and T. Veeraklaew, "Designing robots for optimal performance during repetitive motion," *IEEE Trans. on Robots and Automation*, vol. 14, no. 5, pp. 771-777, Oct. 1998.

[17] T. I. Fossen, *Guidance and Control of Ocean Vehicles*, John Wiley & Sons Ltd., Chichester, 1994.

[18] K. S. Fu, R. C. Gonzalez, and C. S. G. Lee, *Robotics: Sensing, Vision, and Intelligence*, McGraw-Hill, Singapore, 1987.

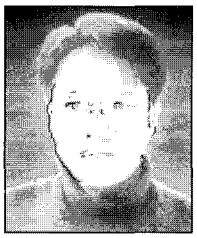

Bong-Huan Jun received the B.S. and M.S. degrees in Mechanical Engineering from Pukyong National University, Busan, Korea, in 1994 and 1996, respectively. He is currently working toward a Ph.D. degree in the Department of Mechatronics Engineering at Chungnam National University, Daejeon, Korea. He joined the Ocean Engineering Research Department of the Maritime and Ocean Engineering Research Institute (MOERI), KORDI in 1996 as a Research Scientist. His research interests include analysis and motion planning of underwater manipulators, navigation guidance and control of underwater vehicles. Mr. Jun is a member of the Institute of Control Automation System Engineers (ICASE) and the Korea Society of Ocean Engineers (KSOE) in Korea.

Jihong Lee received the B.S. degree in Electronics Engineering from Seoul National University, Korea in 1983, and the M.S. and Ph.D. degrees from the Korea Advanced Institute of Science and Technology (KAIST), Daejeon, Korea, in 1985 and 1991, respectively, all in Electrical and Electronics Engineering. Since 2004, he has been a Professor in the Mechatronics Engineering Department of Chungnam National University, Daejeon, Korea. His research interests include robotics, especially robot hand and kinematic analysis, as well as embedded systems. Prof. Lee is a member of the Institute of Control Automation System Engineers (ICASE) and the Institute of Electronics Engineering of Korea (IEEK) in Korea.

Pan-Mook Lee received the B.S. degree from Hanyang University, Seoul, Korea, and his M.S. and Ph.D. degrees from the Korea Advanced Institute of Science and Technology (KAIST), Daejeon, Korea, in 1983, 1985, and 1998, respectively, all in Mechanical Engineering. Since 1985, he has been a Principal Researcher with the Ocean Engineering Research Department of the Maritime and Ocean Engineering Research Institute (MOERI), KORDI, Daejeon, Korea. He was a Visiting Researcher with the University of Hawaii at Manoa between 1998 and 1999. His research interests include navigation, guidance, and control of underwater vehicles, signal processing in the ocean environment, and applications of intelligent underwater vehicles. Dr. Lee is a member of the Institute of Control Automation System Engineers (ICASE) and the Korea Society of Ocean Engineers (KSOE) in Korea. He is also a member of the Automatic Control, Oceanic Engineering, Industrial Electronics, and Robotics and Automation Societies of IEEE, and the International Society of Offshore and Polar Engineers (ISOPE).